

E. F. Schum, J. H. DeHart, and P. M. Bevilaqua
 Rockwell International Corp.
 North American Aircraft Operations
 Columbus, Ohio

Abstract

A combination of computer analysis and scale model testing was utilized to develop a nozzle which would increase the performance of thrust augmenting ejectors. Scale model tests were conducted on various multi-lobed and vortex-generating nozzles. Predicted jet characteristics were obtained by calculating a finite difference solution of Reynolds equations for the three-dimensional flow field. A two-equation turbulence kinetic energy model was used for closure. It is demonstrated that the thrust augmentation of the XfV-12A ejector can be increased from 1.45 to 1.63 by the addition of lobes to the baseline nozzle, and a corresponding increase of throat width.

Introduction

The static thrust of turbojet engines can be significantly increased by diverting the exhaust flow through an ejector pump. According to the laws of momentum and energy conservation, greatest thrust is obtained from a given energy input by accelerating a large mass of air to a low exhaust velocity. Within an ejector, thrust is increased by transferring the kinetic energy of the engine exhaust stream to a larger mass of air drawn from the atmosphere. The ejector duct experiences a reaction force which is equal but opposite to the momentum change of the accelerated stream. Details of this process have been discussed by Bevilaqua.⁽¹⁾

The mechanism of this energy transfer is the turbulent mixing of the two streams. Thus, increases in ejector thrust augmentation can be obtained by increasing the turbulent mixing rate. Appreciable increases in mixing and augmentation have been achieved with the so-called hypermixing nozzles.^(2,3) The alternating exit of the hypermixing nozzle serves to introduce a row of stream-wise vortices into a plane jet (Figure 1).

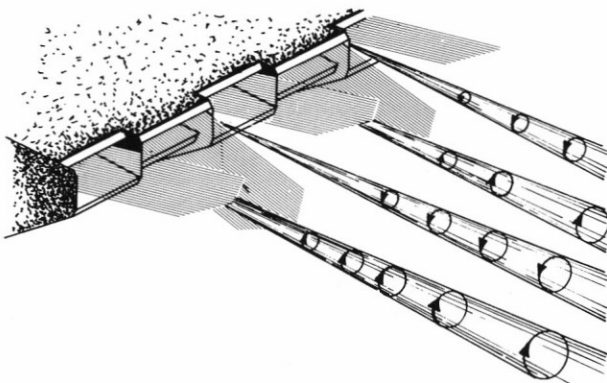


Figure 1. Hypermixing Nozzle Exit

These vortices serve to accelerate the turbulent mixing and thereby entrain additional fluid into the ejector. Because of the favorable entrainment characteristics of the hypermixing nozzles, they were used in the centerbody of the XfV-12A airplane. In a recent study⁽⁴⁾ of potential V/STOL configurations, ejectors were also used in the wing section (Figure 2).

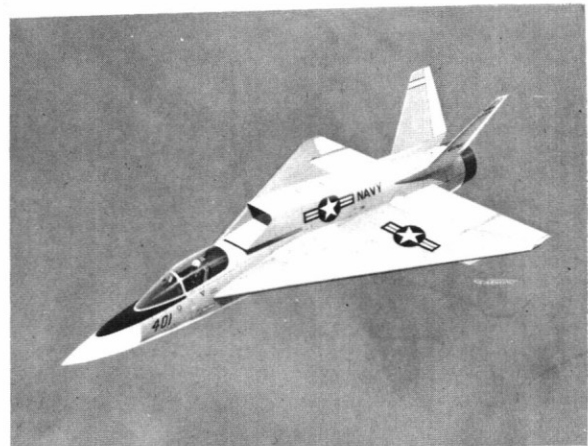


Figure 2. V/STOL Configuration

Figure 3 illustrates schematically how the ejector components fold into the shape of a wing for forward flight. This study is concerned with the development of the centerbody nozzle.

The specific objective of this investigation was to develop and demonstrate centerbody nozzles that would provide increased augmentation exceeding the peak value of 1.45 obtained for the hypermixing configuration.

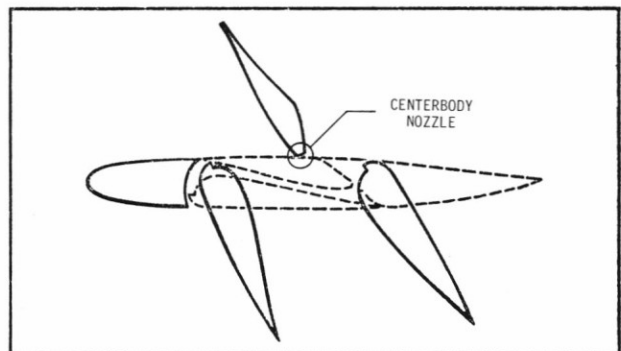


Figure 3. Deflected Ejector Wing

In the following sections, a "master plan" is presented in which a three-dimensional, turbulent kinetic energy program is used to calculate the turbulent mixing. Analytical and experimental results for both symmetric and asymmetric, centerbody nozzle configurations are discussed.

Nozzle Development Plan

The overall plan consisted of three phases.

Phase I To Improve Analytical Capability for Calculating Three-Dimensional Turbulent Flow by:

- o Identifying inlet turbulence kinetic energy properties for ejectors (k, ϵ)
- o Developing an inlet grid generation program
- o Simplifying, using incompressible flow

Phase II To Compare Analyses with Experiment for Hypermixing Nozzles to Update Analytical Technique

Phase III To Develop and Demonstrate Centerbody Nozzles that Increase Augmentation

Analytical Model and Numerical Approach

Turbulent Kinetic Energy Program

In brief, the turbulent flow equations and numerical methods, developed by Patankar and Spalding,⁽⁵⁾ were used in this study. This afforded a considerable saving in both computer storage and running time. In their method, the solution of the original boundary value problem is reduced to an initial value problem which may be solved by streamwise marching procedures. Since there is a primary direction of flow (through the ejector), the streamwise velocity component is considered to be driven by a mean pressure, $\bar{P}(X)$, which is decoupled from the perturbation pressures, $P'(X,Y,Z)$, in the transverse plane.

The turbulent stresses are related to the mean velocity gradient according to the usual eddy viscosity assumption, Schlichting.⁽⁶⁾ The eddy viscosity is calculated using the two-equation, turbulent kinetic energy model of Launder and Spalding.⁽⁷⁾ According to this model, the eddy viscosity is assumed to be a function of the turbulent kinetic energy, k , and its rate of dissipation, ϵ . Values of the turbulence constants, suggested by Launder and Spalding⁽⁷⁾ were used.

The basic differential equations are put in finite difference form by integrating them over a control volume surrounding a typical grid point. A more complete description of this procedure and an illustration of its use has been given by DeJooode and Patankar.⁽⁸⁾

Boundary Conditions

Figure 4 presents a typical ejector configuration, containing a hypermixing centerbody nozzle. Other types of centerbody nozzle designs can also be analyzed.

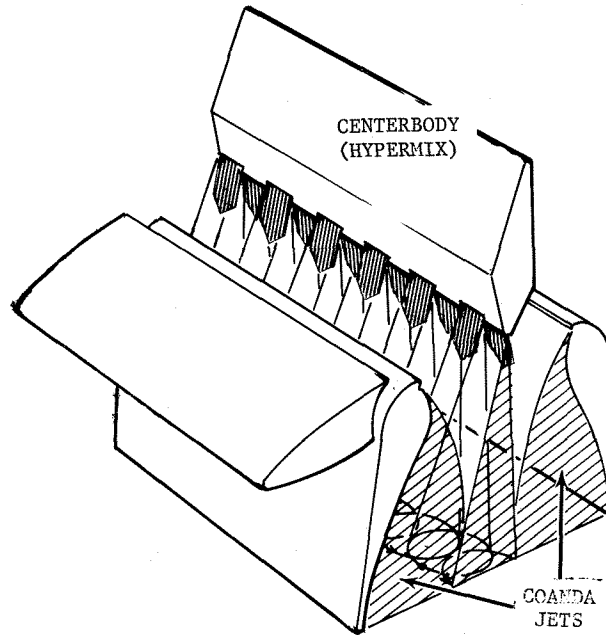


Figure 4. Typical Ejector Wing Configuration

The computational boundaries are outlined in Figure 5 for the hypermixing nozzle. Symmetry planes are used as computational boundaries in the spanwise direction because most nozzle designs are periodic along the span. The two ejector walls form the other boundaries. From these boundaries and the specified primary flow area, the ejector geometric parameters can be calculated. These parameters include the throat to inlet primary flow area, A_2/A_0 , the ejector exit to throat area, A_3/A_2 , and the diffuser length to throat width, L/D .

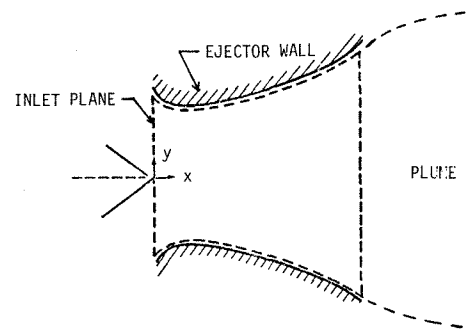
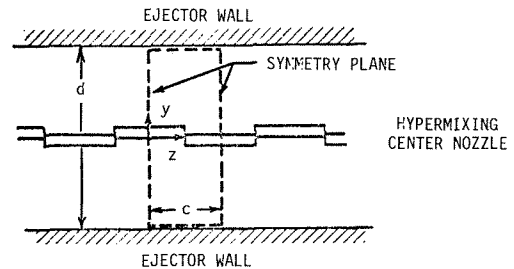


Figure 5. Computational Boundaries

Initial Conditions

Since the differential equations are solved in the program by a streamwise integration, initial values of all of the flow variables must be specified in order to start the calculation. Primary nozzle jet velocities are calculated for the given pressure ratio from the conventional isentropic relation using a velocity coefficient of 0.925.⁽⁹⁾ Because most of the nozzles studied employ some jet deflection to generate hypermixing type vortices, the initial, calculated jet velocity vector is inclined to the ejector axis. Thus, the predictions of ejector thrust augmentation due to increased mixing are balanced against the tilt loss in the primary jet thrust. Secondary stream velocities are obtained from Bernoulli's equation using the inlet mean static pressure along with the ambient pressure. The mean static pressure is obtained in the iterative solution of the viscous flow field and is discussed in the "Closure Scheme." The angularity of the secondary stream velocities was measured at the inlet plane in the chordwise and spanwise direction. This is shown schematically in Figure 6. These data were generalized and incorporated into the program.

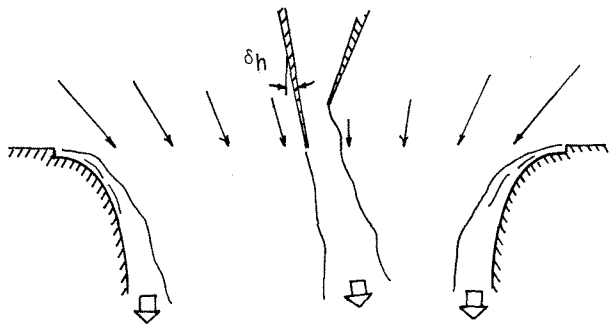


Figure 6. Measured Inlet Velocities

The initial value of the turbulence kinetic energy is expressed as a fraction of the mean flow energy,

$$k = C_k U_j^2$$

and the initial dissipation rate is assumed to be proportional to the rate of energy addition by the jet

$$\epsilon = C_\epsilon U_j^3 / t$$

in which U_j and t are the initial values of the jet velocity and width.

A value of 0.04 was used for C_k . Based on the data presented by Rodi,⁽¹⁰⁾ this value corresponds to the average of that for self-similar mixing layers and planar jets. Hot film measurements, made for the hypermixing nozzles, confirmed this value. A value of 0.0027 was used for C_ϵ based on the data in Hinze⁽¹¹⁾ for the turbulent flow in pipes.

Inlet Grid Generator

At the inlet computational plane of the ejector, it is necessary that the flow area be subdivided into a grid of approximately 1500 to 3000 control areas (volumes) with corresponding velocities (primary or secondary). To reduce the usual 20 hour setup time to less than an hour and also eliminate the arbitrariness of the subdivision, a computer program was written to generate the grid. For the grid program, only the ejector and nozzle dimensions are the primary input. A grid for the hypermixing configuration contains approximately 3000 control volumes (Figure 7). At the upper and lower surfaces, the grid appears to be shaded because in the Coanda jet region, a much finer grid is used.

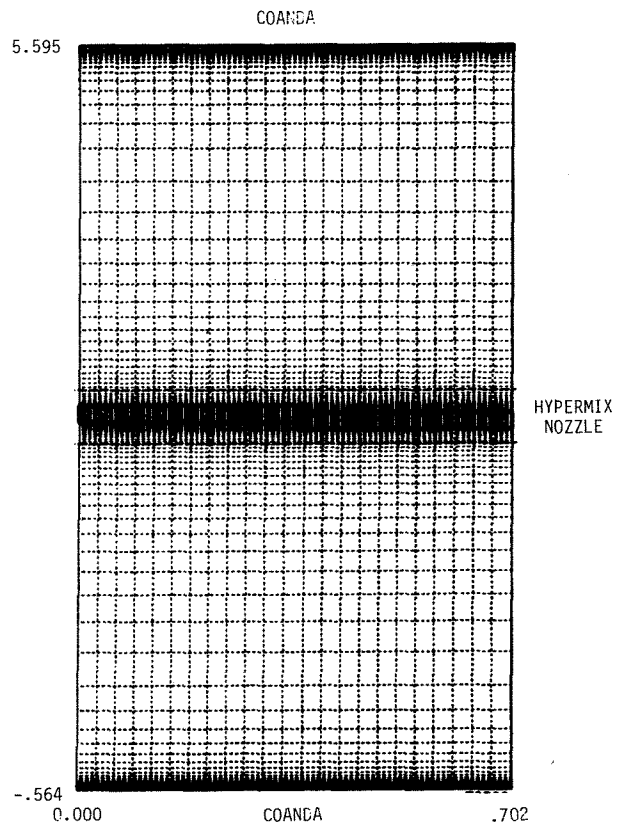


Figure 7. Computational Grid for Hypermixing Centerbody Configuration

Closure Scheme

Closure is obtained by iterating on the inlet pressure (secondary flow) until the calculated pressure at the end of the exhaust plume is ambient. The plume exit pressure is dependent upon the curvature of the jet sheet leaving the trailing edge of the ejector shroud as well as the plume length. Both the curvature and plume length are determined by the difference between the ambient pressure and the ejector exit pressure. This "jet flap" effect is discussed in more detail by DeJode and Patankar.⁽⁸⁾

The thrust augmentation ratio, ϕ , is defined to be the ratio of the ejector stream thrust to the isentropic thrust obtained by expanding the same mass of primary fluid (\dot{m}_{pri}) to atmospheric pressure. The thrust of the ejector is evaluated by integrating the exit momentum flux and pressure force,

$$T = \int_{A_3} \rho U^2 dY dZ - (P_\infty - P_3)A_3$$

in which P_3 and A_3 are the static pressure and area at the exit. ϕ is defined as:

$$\phi = \frac{T}{\dot{m}_{pri} U_{isent}}$$

As noted later, curvature effects were not included in the modeling of the Coanda flow, thereby affecting the value of the calculated ϕ 's. Thus, when comparing ejector performance, the difference in ϕ is used instead of comparing the absolute values of ϕ .

Simplification for Incompressible Flow

To reduce computer time, the analysis was conducted using the incompressible option in the program. With this, density is assumed constant and the state and energy equations are bypassed. To verify that this was a valid approach, both compressible and incompressible computer runs were made for a hypermixing configuration at a pressure ratio of 2.2 and a primary gas temperature of 80°F (usual test conditions). There was little difference in the calculated ejector exit velocity profiles. This simplification afforded a saving of about 30 percent or 10 minutes of CPU time on the CDC-176 computer.

Results and Discussion

The following sections describe how the hypermixing test results interacted with the computer program development (Phase II) so that it could be used to identify higher performance symmetric and/or asymmetric nozzle configurations (Phase III).

Hypermixing Nozzles

Two geometric parameters that can affect ϕ are the aspect ratio of the hypermixing nozzle slots and the hypermixing angle. Salter's(12) data for aspect ratios of 4 to 12 showed that the aspect ratio did not have a large effect on the entrainment (and hence augmentation) of the ambient air into the jet. Calculated ϕ 's, obtained with the computer program, confirmed this. The effect of the hypermixing angle was analytically studied because of the lack of data. It was necessary, however, to first assess the accuracy of the analytical model by comparing calculated and measured velocities.

Figure 8 presents the calculated and measured two-dimensional main stream velocity distribution at the ejector exit for two lateral positions. These positions correspond to the middle of the hypermixing element and between adjacent elements.

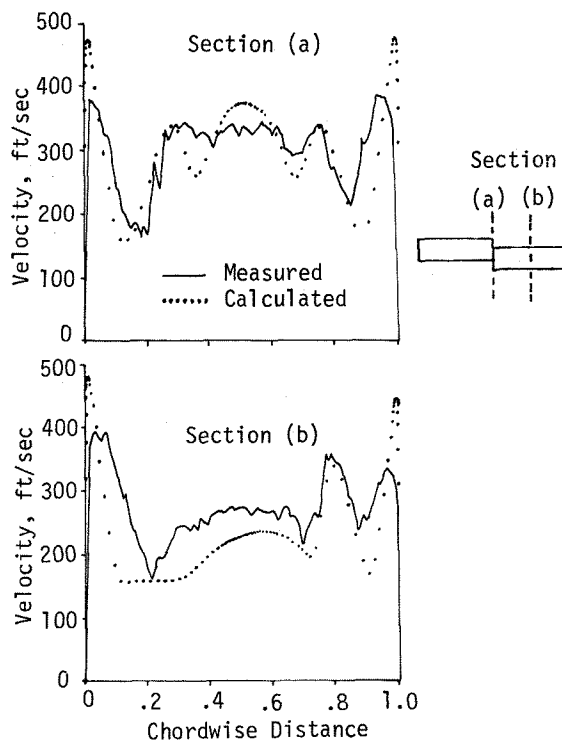


Figure 8. Comparison of Calculated and Measured Velocity Profiles at Ejector Exit for 15° Hypermixing Nozzles

In general, the agreement is good. However, as previously noted, Coanda curvature effects have not been included in the analysis.

The effect of the hypermixing angle on the three-dimensional, calculated velocity distribution at the ejector exit is shown in Figure 9. Velocities

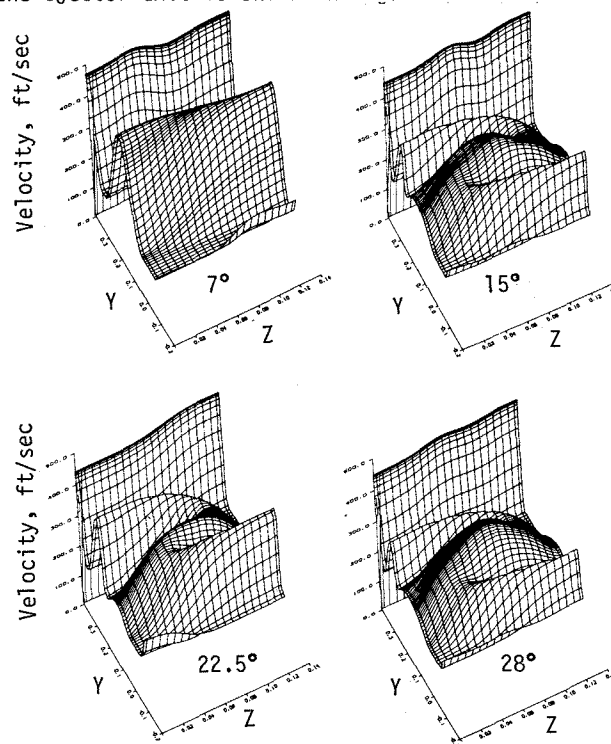


Figure 9. Effect of the Hypermixing Angle on Calculated Velocities at Ejector Exit

are for hypermixing angles of 7, 15, 22.5, and 28° and for a pressure ratio of 2.2. The Coanda jet in the foreground was purposely omitted from the plot in order that the hypermixing velocity distribution could be seen. With increasing hypermixing angles, the vortex action is increased, evident by the flattening of the center jet velocity profiles.

The effect of these hypermixing angles on the predicted values of ϕ is shown in Figure 10. Analytical results were normalized at a ϕ of 1.45 at 7°. This reference value corresponds to the ϕ measured for the 7° hypermixing nozzle configuration, used in the XFV-12A airplane. The results are for an $A_2/A_0 = 16.2$, $A_3/A_2 = 1.9$, and an $L/D = 1.8$. Because the analytical results predicted an increase in ϕ with hypermixing angle, model tests were conducted to verify the predicted trends. Up to about 20°, the predicted trend agreed with measured values. Beyond 20°, calculated ϕ 's decreased while the measured values remained essentially constant. The lack of agreement beyond about 20° is attributed to an assumption used to simplify the flow equation: that the V and W velocity components are much smaller than the mainstream velocity, U. At high deflection angles, this may not be true.

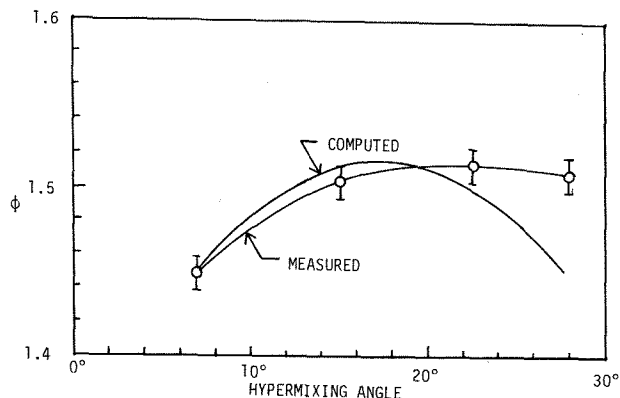


Figure 10. Comparison of Measured and Computed Augmentation

These results demonstrated that the measured ϕ could be increased from the original value of 1.45 to 1.51 by increasing the jet deflection angle as analytically predicted. Because of the good agreement of calculated and measure velocities along with the general ϕ trends, the program was used in the design and analyses of other nozzle configurations. This is the subject of the following sections.

Symmetric Nozzles

Measurements by Mefferd, et al.⁽¹³⁾ showed that when the primary nozzles are made to extend further across the inlet plane (parallel to the symmetry plane in Figure 5), than that for hypermixing nozzles, ϕ was increased. Figure 11 shows such a configuration, consisting of a series of symmetric cross slots. The downstream vortex action is shown schematically.

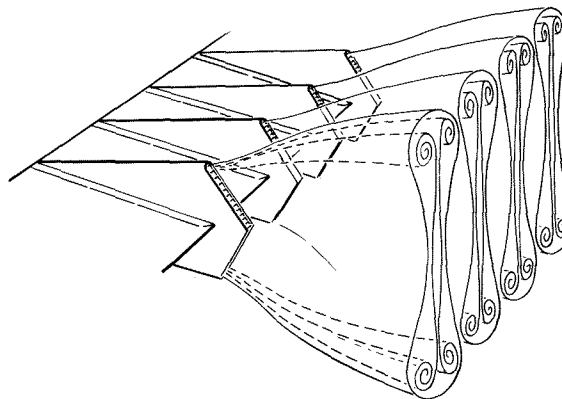


Figure 11. Symmetric Cross Slot Flow Pattern

In Figure 12, a span slot extending between the cross slots has been added. In this configuration the thickness of the cross slot gap is shown to increase linearly from the centerline. In other configurations this thickness is held constant.

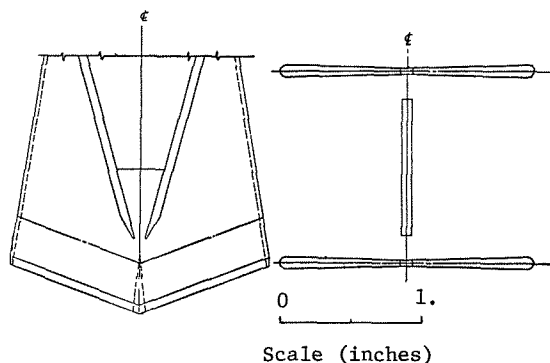
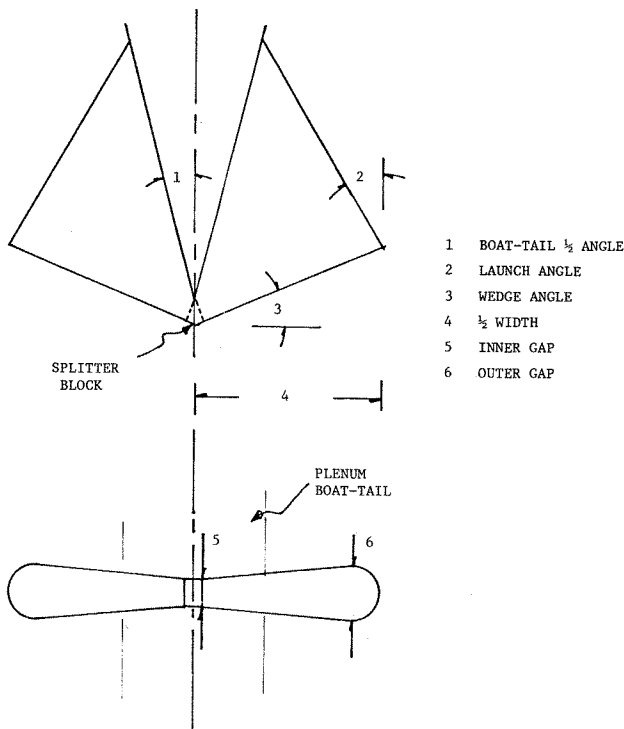


Figure 12. Typical Cross Slot-Span Slot Configuration

Parameters that affect the performance of such nozzles include the bowtie ratio, cross slot-span slot flow split, cross slot aspect ratio and the cross slot primary flow discharge angle. The geometric parameters are shown in Figure 13. The effect of these parameters on ejector performance is discussed in the following paragraphs.

Bowtie Ratio: A "bowtie nozzle" shape (cross slot nozzle gap varying, as shown in Figure 12) should increase entrainment and, hence, ϕ by placing more primary flow into the "dog bone" vortices at the cross slot tips (Figure 11). Analytical results are compared with experimental results in Figure 14. Up to a bowtie ratio of about 2, ϕ does increase as predicted.

Cross Slot-Span Slot Flow Split: Analytical and experimental tests were conducted with the cross slot-span slot configurations to determine the effect of flow split. Flow split is defined as the ratio of the flow through the span slots to the total primary flow. Results are compared with data in Figure 15. Best performance is obtained when the flow to the span slot is about 40 percent or less. These results are understandable since the downstream jet expansion from the span slot can generate destructive interference with the flow from the cross slot.



BOWTIE RATIO = OUTER GAP/INNER GAP
 CROSS SLOT ASPECT RATIO = $(\text{WIDTH} - \text{SPLITTER})^2 / \text{AREA}$

Figure 13. Cross Slot Geometric Parameters

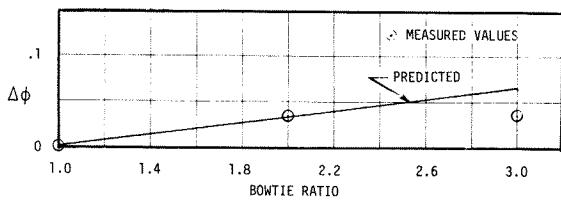


Figure 14. Effect of Bowtie Ratio

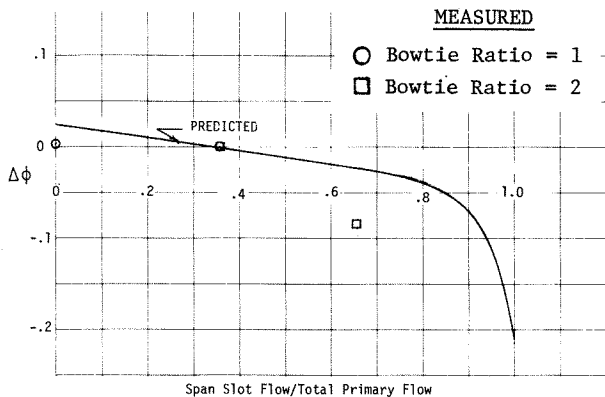


Figure 15. Effect of Flow Split

Cross Slot Aspect Ratio: Since the results in the previous section showed that the percent primary flow to the cross slot nozzle should be increased, the next logical step was to investigate the effect of cross slot aspect ratio. Earlier work by Salter⁽¹²⁾ showed that the entrainment for two-dimensional free jets is increased with aspect ratio. Predicted results for augmenters (Figure 16) show that $\Delta\phi$ is increased with cross slot aspect ratio; however, physical width constraints must be considered.

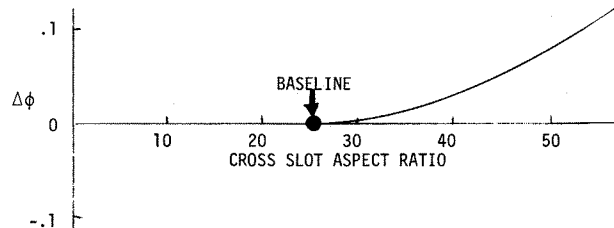


Figure 16. Effect of Cross Slot Aspect Ratio

Cross Slot Primary Flow Discharge Angle: The hypermixing nozzle studies, both test and analysis, had identified that the initial jet flow angle was a primary factor in ejector performance. The flow angles generated by the hypermixing nozzles were directly related to the angle of the slots and were easily known, a priori, for both tests and analysis. Correlation and/or nozzle design was therefore rather straightforward. However, the cross slot type nozzles presented a problem in that the relationship between flow angle and geometry was not usually known. Therefore, tests were conducted to determine the dependence of flow angle on nozzle geometry. A parallel analytical study was conducted (using the computer program) to determine the effect of jet flow angle on augmentation ratio. Correlation of the two studies resulted in a capability to define the nozzle geometry required to obtain the desired augmentation ratio. The results of these studies are presented in this section.

Figure 17 presents the angularity data for four nozzle configurations having the following wedge and launch angles: (a) 0° , 21° ; (b) 21° , 21° ; (c) 11° , 17.2° ; and (d) 21° , 9° . Schematics of the corresponding nozzles are also shown. The abscissa is the nondimensional distance from the centerline to the edge of the nozzle. Measurements were made under four nozzles in each configuration. For this reason there is some scatter due to slight manufacturing differences for the small scale model augmenters, evident in Figure 17(c). For analytical purposes, the profile shapes were approximated by straight lines. Calculated $\Delta\phi$'s are shown in Figure 18 for a linearly varying and for a constant angular distribution. The $\Delta\phi$'s are referenced to a baseline configuration having a 0° wedge and launch angle. The abscissa is the average of the angle at $S = 0$ and $S = 1$. Analytical results show that a nozzle having the linearly varying flow angle provides a greater $\Delta\phi$.

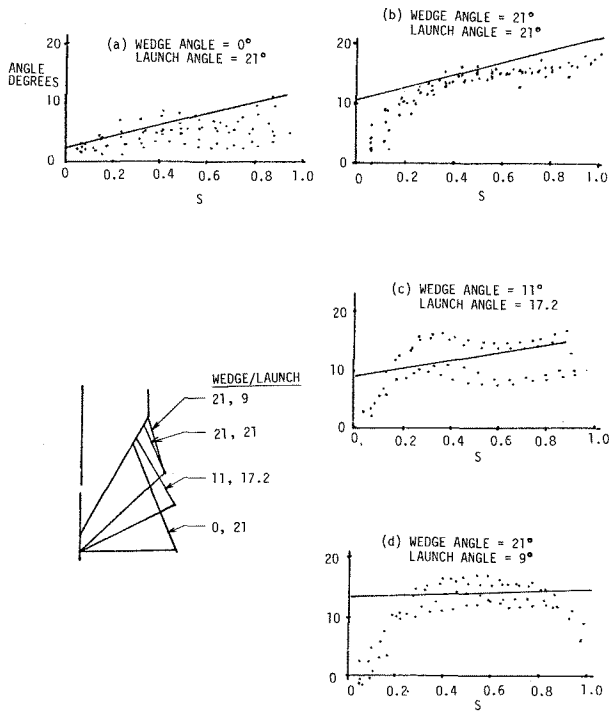


Figure 17. Cross Slot Nozzle Exit Flow Angles

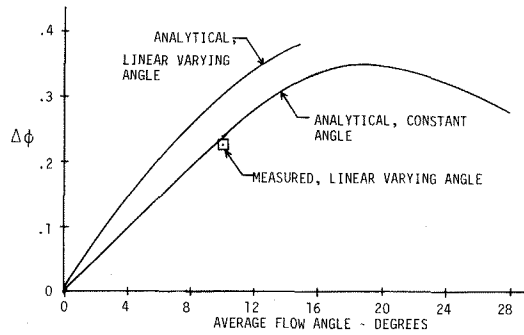


Figure 18. Effect of Constant and Linearly Varying Cross Slot Exit Angularity on $\Delta\phi$

The results of the combined analytical/experimental jet angle studies were used to design a nozzle capable of a linear jet angle variation (Figure 19). Figure 20 presents a comparison of

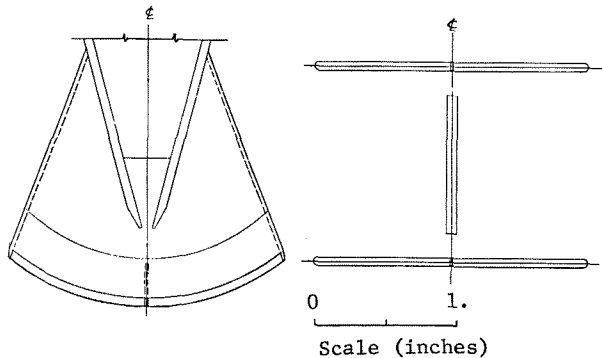


Figure 19. Cross Slot-Span Slot Nozzle with a Linearly Varying Exit Profile

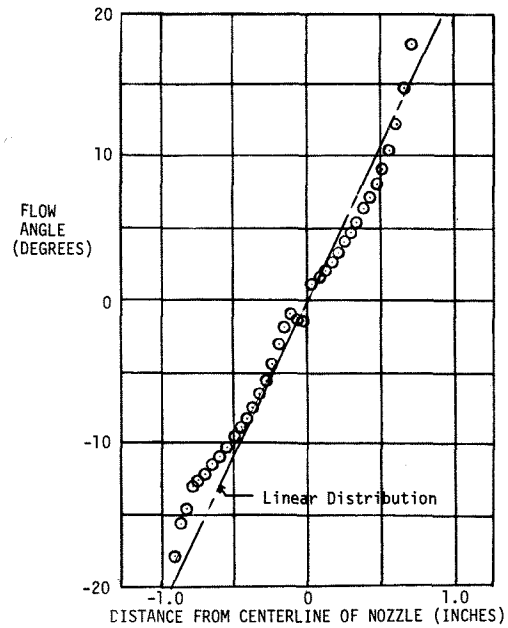


Figure 20. Measured Flow Angles for Linearly Varying Slot Nozzle Configuration

the measured flow angularity with the desired linear distribution. The results demonstrate that a nozzle can be designed to provide a desired angular distribution. For this configuration (average flow angle of 10°), the predicted $\Delta\phi$ was 0.30 while the measured value was 0.24 (Figure 18).

Symmetric Nozzle Overall Performance: By combining the computer analysis with the tests of the inlet flow angularity, geometric variations, etc., a cross slot-span slot nozzle was designed to improve augmentation (Figure 19). A measured peak ϕ of 1.63 was obtained as shown in Figure 21 for an

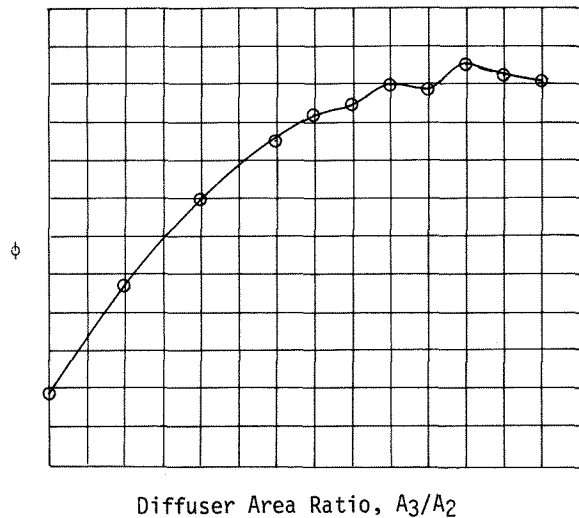


Figure 21. Measured Thrust Augmentation for Cross Slot-Span Slot Nozzle Having a Linearly Varying Exit Velocity Profile

A_2/A_0 of 19.6 and an L/D of 1.5. For the hypermixing nozzles, the corresponding values are 16.2 and 1.8. Since these cross slot nozzles produced more entrainment than the hypermixing nozzles, a larger inlet area ratio could be used to further increase the augmentation. This effect was discussed by Bevilaqua.(1)

Asymmetric Nozzles

This type nozzle was developed in an effort to capitalize on the generally superior entrainment characteristics of the symmetric cross slot nozzle configuration while maintaining packaging limits imposed by supersonic airfoil contours. The design combines a series of aft facing, spanwise slot nozzles with an alternating series of cross-slots on the forward side. Measured ϕ performance, however, was between that for the hypermixing nozzles and the symmetric, cross slot-span slot nozzle with the linearly varying exit discharge angle.

Conclusions

The following results were obtained from a combined analytical and experimental investigation of centerbody nozzle configurations.

- By combining the data of hypermixing nozzle configurations with a three-dimensional, turbulent kinetic energy computer program, an analytical procedure was developed for predicting the flow field in ejectors and their augmentation, ϕ .
- The measured ϕ for the 7° hypermixing nozzle, used in the XFV-12A airplane, was 1.45. It was analytically and experimentally shown that a peak ϕ of 1.51 could be obtained by increasing the hypermixing angle to 22°.
- Analytical and test results showed that the parameters affecting ϕ include the throat width, bowtie ratio, relative flow to the cross slot, cross slot aspect ratio, and the cross slot exit velocity angularity.
- By combining the computer program with test data of inlet flow angularity, geometric variations, etc., a measured peak ϕ of 1.63 was demonstrated for the cross slot-span slot configuration in which the exit angularity of the cross slot varied linearly with distance.

References

1. Bevilaqua, P. M., "Lifting Surface Theory for Thrust-Augmenting Ejectors," AIAA Journal, Vol. 16, No. 5, May 1978, pp. 475-481.
2. Quinn, B. P., "Compact Ejector Thrust Augmentation," Journal of Aircraft, Vol. 10, No. 8, August 1973, pp. 481-486.
3. Bevilaqua, P. M., "Evaluation of Hypermixing for Thrust Augmenting Ejectors," Journal of Aircraft, Vol. 11, No. 6, June 1974, pp. 348-354.

4. Mark, L., "Study of Aerodynamic Technology for Single-Cruise Engine V/STOL Fighter/Attack Aircraft," NASA CR166270, January 1982.
5. Patankar, S. V. and Spalding, D. B., "A Calculation Procedure for Heat, Mass and Momentum Transfer in Three-Dimensional Parabolic Flows," Int. J. Heat Mass Transfer, Vol. 15, 1972, pp. 1787-1806.
6. Schlichting, H., "Boundary Layer Theory," 6th Ed. McGraw-Hill Book Co., 1968.
7. Launder, B. E. and Spalding, D. B., "The Numerical Computation of Turbulent Flows," Computer Methods in Applied Mechanics and Engineering, Vol. 3, No. 2, March 1974, pp. 269-289.
8. DeJoode, A. D. and Patankar, S. V., "Prediction of Three Dimensional Turbulent Mixing in an Ejector," AIAA Journal, Vol. 16, No. 2, February 1978, pp. 145-150.
9. Mefferd, L. A. and Bevilaqua, P. M., "Computer-Aided Design Study of Hypermixing Nozzles," NR78H-91, NASC Contract N00019-77-C-0527, July 1978.
10. Launder, B. E., "Studies in Convection, Theory, Measurements, and Applications," Vol. 1, Academic Press, 1975.
11. Hinze, J. O., "Turbulence," McGraw-Hill Book Co., 1959.
12. Salter, G. R., "Mass Entrainment by Hypermixing Jets," Bell Aerospace Division of Textron, ARL TR75-0132, June 1975.
13. Mefferd, L. A., Alden, R. E., and Bevilaqua, P. M., "Design and Test of a Prototype Scale Ejector Wing," Workshop on Thrust Augmenting Ejectors at Ames Research Center, June 28-29, 1978, NASA Conference Publication 2093, September 1979.